Transition from electron accumulation to depletion at β-Ga_2O_3 surfaces: The role of hydrogen and the charge neutrality level

J. E. N. Swallow,[1,a)] J. B. Varley,[2] L. A. H. Jones,[1,3] J. T. Gibbon,[1] L. F. J. Piper,[4] V. R. Dhanak,[1] and T. D. Veal[1,b)]

[1)] *Stephenson Institute for Renewable Energy and Department of Physics, University of Liverpool, Liverpool L69 7ZF, UK.*
[2)] *Lawrence Livermore National Laboratory, Livermore, California 94550 USA.*
[3)] *Department of Electrical Engineering and Electronics, University of Liverpool, Brownlow Hill, Liverpool L69 3GJ, UK.*
[4)] *Department of Materials Science and Engineering, Binghamton University, Binghamton, New York 13902, USA.*

The surface electronic properties of bulk-grown β-Ga_2O_3 ($\bar{2}01$) single crystals are investigated. The band gap is found using optical transmission to be 4.68 eV. High-resolution x-ray photoemission coupled with hybrid density functional theory calculation of the valence band density of states provide insights into the surface band bending. Importantly, the standard linear extrapolation method for determining the surface valence band maximum (VBM) binding energy is found to underestimate the separation from the Fermi level by ~0.5 eV. According to our interpretation, most reports of surface electron depletion and upward band bending based on photoemission spectroscopy actually provide evidence of surface electron accumulation. For uncleaned surfaces, the surface VBM to Fermi level separation is found to be 4.95±0.10 eV, corresponding to downward band bending of ~0.24 eV and an electron accumulation layer with sheet density of $\sim 5 \times 10^{12}$ cm^{-2}. Uncleaned surfaces possess hydrogen termination which act as surface donors, creating electron accumulation and downward band bending at the surface. In situ cleaning by thermal annealing removes the H from the surface, resulting in a ~0.5 eV shift of the surface VBM and formation of a surface electron depletion layer with upward band bending of ~0.26 eV due to native acceptor surface states. These results are discussed in the context of the charge neutrality level, calculated bulk interstitial hydrogen transition levels, and related previous experimental findings.

Beta phase gallium oxide (β-Ga_2O_3) is a transparent, oxide semiconductor material that has attracted a large amount of interest in recent years due in part to its wide band gap (~4.7eV at room temperature),[1,2] gas adsorption-tunable conductivity, and high breakdown field (8 $MVcm^{-1}$). These properties mean that β-Ga_2O_3 is a promising material for a large range of applications, such as solar-blind ultraviolet photodetectors[3], gas sensing devices,[4] and high power electronic devices.[5] Despite the suitability of this material for such a large range of applications, there is a distinct lack of spectroscopic information on its surface electronic behavior. Unlike other oxide semiconductors, such as In_2O_3 [Ref. 6], SnO_2 [Ref. 7], CdO [Ref. 8] and ZnO [Ref. 9], the surface electronic behavior has not been well understood in the case of Ga_2O_3, which is an important factor for gas sensing devices and electronic contacts.

Semiconductors with the greatest mismatch between their cation and anion in terms of atomic size and electronegativity, such as CdO [Ref. 8,10] and In_2O_3 [Refs 6,11] and InN [Ref. 12,13], appear to only exhibit surface electron accumulation, as opposed to the electron depletion present at the surface of the majority of n-type semiconductors.[14] The slightly less mismatched materials such as ZnO [Refs 15–18] and SnO_2 [Refs 19,20] can have either of these two types of surface space charge, depending on how the surface is treated. Indeed,

[a)]Electronic mail: JackSwallow@outlook.com
[b)]Electronic mail: T.Veal@liverpool.ac.uk

it has been proposed recently that electron depletion is the inherent space charge property of the ZnO surface.[17,18]

As the Ga cation is smaller and has higher electronegativity than Zn, such a trend suggests that Ga_2O_3 may behave, in terms of surface space charge properties, more like ZnO than In_2O_3. Upward surface band bending and electron depletion is assumed in Ga_2O_3 due to the difficulty in achieving Ohmic contacts with low conductivity material,[21] consistent with similar observations for ZnO. In this context, recent x-ray photoemission spectroscopy (XPS)[22–24] and angle resolved photoemission spectroscopy (ARPES)[25–27] has been interpreted as indicating surface electron depletion and upward band bending. However, previous analysis of XPS valence band spectra employed the method of linear extrapolation of the leading valence band edge which underestimates the surface valence band maximum (VBM) to Fermi level separation. This is because, just as in the case of In_2O_3,[6] the top of the valence band has very little dispersion and a high effective mass, leading to a very rapid onset of the density of states. Instrumental broadening in XPS introduces a significant slope to the measured onset of the valence-band photoemission, leading to the aforementioned underestimation. In the case of the previous ARPES data where the resolution is higher, the broadening is lower and so a higher surface VBM to Fermi level separation has been reported of about 4.9–5.0 eV. However, the presence of electron depletion was still incorrectly inferred due to a band gap of about 4.9 eV being assumed, higher than the measured room temperature value, some 0.2 eV or so lower.[25–27]

Further, the space charge layer of the ZnO surface has been shown to be highly dependent on surface properties,[15,16] especially the effects of H adsorption.[28] Whilst H doping in the bulk has been considered in recent years for Ga_2O_3 both experimentally[29] and theoretically,[30,31] its influence on the surface has mainly been considered from a gas sensing perspective in terms of changes to the measured conductivity,[32,33] rather than in photoemission studies. Here we report the surface electronic behavior and band bending of β-Ga_2O_3, and contrast our interpretation of XPS data with that contained in other recent reports.

Bulk single crystalline $(\bar{2}01)$ β-Ga_2O_3 (from Novel Crystal Technology, Inc., Tamura Corporation) grown using the edge-defined film-fed growth method[34] was used in this study. Sn-doped samples were used to make them sufficiently conducting to avoid sample charging effects during photoemission measurements. The net donor density ($N_D^+ - N_A^-$) was determined by capacitance-voltage measurements to be 6×10^{18} cm^{-3} and the free electron density was confirmed to be n$\sim6\times10^{18}$ cm^{-3} using Hall effect measurements. Optical transmittance was performed using a Shimadzu UV-Vis-IR 3700 spectrophotometer which employs a photomultiplier detector to reach energies up to 6.5 eV, enabling the absorption onset of β-Ga_2O_3 to be determined. XPS was performed using a SPECS monochromatic Al Kα ($h\nu$ =1486.7 eV) x-ray source operated at 250 W. A PSP Vacuum Technology hemispherical electron-energy analyzer with a 120 mm mean radius was employed to detect photoelectrons, operated at a pass energy of 10 eV (50 eV for survey scans). The XPS system is described in detail elsewhere.[35] Binding energies are stated throughout with respect to the Fermi level. Binding energies are calibrated using the Fermi edge of an Ar^+-ion bombarded polycrystalline silver sample, also enabling the resolution of 0.4 eV to be determined. This resolution includes broadening due to the x-ray source, the electron analyser and thermal effects. The uncertainty in stated binding energies is $\pm$0.05 eV. All measurements were performed at room temperature. Prior to in-situ cleaning, the Ga_2O_3 was investigated in its as-received form. In-situ surface cleaning was performed via sample annealing at between 200 and 800°C for 30 min cycles[23,36,37] and a final 2 hour cycle at 800°C.

Our modelling adopts the HSE06 screened hybrid functional[38,39] and projector-augmented wave (PAW) approach[40] as implemented in the VASP code.[41,42] We explicitly include the semi-core Ga 3d states as valence electrons and adopted a fraction of 32% exact-exchange in the hybrid functional. These choices lead to an excellent description of the lattice and electronic structure, with a 0 K direct gap of 4.87 eV (indirect of 4.86 eV).[43] Temperature effects lead to a decrease of $\sim$0.2 eV between 0 K and room temperature according to recent measurements.[44] The treatment of the Ga d states leads to slightly improved

lattice parameters as compared to experiment (12.21, 3.03, and 5.79 Å for the a, b, and c lattice parameters, and a β angle of 103.8 degrees), and most importantly for this study, an improved description of orbital interactions that can influence the valence band features observable via photoemission spectroscopy. While the primitive unit cell was used for the bulk electronic structure calculations, defect calculations of H_i defects were performed in 120-atom supercells for the Ga_2O_3 and 216-atom supercells for SnO_2 and corrected for finite-size effects following the approach of Freysoldt et al. as described elsewhere.[30,45,46]

In order to determine the band bending at the surface of β-Ga_2O_3 and its evolution with annealing, XPS has been used to measure the valence band and core level spectra at each annealing stage. The valence band spectra give the surface VBM to Fermi level separation. The bulk CBM to Fermi level separation can be determined using semiconductor statistics from the bulk carrier density and, with knowledge of the band gap, this gives the bulk VBM to Fermi level separation. The difference between the bulk and surface VBM energies with respect to the Fermi level thus provides the sign and magnitude of the surface band bending. Changes in the band bending as a function of annealing result in changes to the VBM binding energy with respect to the Fermi level and can be confirmed by observing the corresponding shifts of the core level peaks. The core levels provide additional information about contamination via both peaks due to adsorbed species and chemical shifts of the elements of the semiconductor.

The valence band spectra for β-Ga_2O_3 are shown in Fig. 1 for the sample (a) before surface cleaning, (b) after an 800°C anneal for 2 hours, and (c) the evolution of the valence band over the whole cleaning procedure. The calculated hybrid DFT valence band density of states (VBDOS) are compared to the XPS valence band spectra. Photoionization cross-section corrections taken from Ref. 47 have been applied to the calculated VBDOS with the result shown in Fig. 1 with and without instrumental (0.4 eV full width at half maximum (FWHM) Gaussian) and lifetime broadening (0.45 eV FWHM Lorentzian). The calculated and thus corrected VBDOS is in extremely good agreement with the experimental data.

The methodology of extracting the valence band position is demonstrated in Fig. 1(a) and (b) which involves shifting the broadened calculated VBDOS until it aligns with the spectral features of the XPS data. The leading edge of the unbroadened VBDOS is then taken as the VB-edge position (relative to the Fermi level aligned to zero). This method of determining the VBM energy with respect to the Fermi level is well established[48] but not widely used and the much simpler method of linear extrapolating the leading edge is generally preferred and has been widely used for the analysis of Ga_2O_3 XPS data.[23,49,50] However, as discussed above, for materials with very flat valence bands, with a correspondingly sharp onset of the VBDOS, the linear extrapolation method underestimates the VBM to Fermi level separation due to the instrumental broadening. Comparing the green dotted linear extrapolations in Fig. 1(a) and (b) to the red lines of the aligned unbroadened DOS onset, enables us to determine that linear extrapolation underestimates the VBM position by ~ 0.5 eV. All the calculated VBDOS features match very well with the Ga_2O_3 data, giving good confidence that the VB position is well represented. For materials, such as ZnO, where the valence band onset is more gradual, the two methods for determining the VBM position are in much closer agreement with each other.

Focusing now on Fig. 1(c), it is apparent that after each annealing step the VB edge shifts to lower binding energy. From the valence band spectra, the surface VBM to Fermi level separation is found to vary from 4.95 ± 0.10 eV after no surface preparation to 4.45 ± 0.10 eV after surface cleaning using the highest temperature annealing (800°C).

As mentioned above, to use photoemission to determine the sign and amount of band bending at the polar β-Ga_2O_3 $(\bar{2}01)$, it is important to have a measure of the band gap of the material investigated. Fig. 2 shows two absorption spectra of β-Ga_2O_3 derived from transmission data taken with the crystal oriented perpendicular to each other (schematically shown in inset). A linear extrapolation indicates the onset of optical absorption is at 4.68 eV. This is consistent with other optical measurements[44] energy loss spectroscopy[50] and our calculation results mentioned above. This allows us to give a conservative estimate of the band gap of $\sim4.7\pm0.2$ eV when excitonic effects and optical anisotropy are considered.[1,51]

It also is worth noting the relative independence of band gap on carrier concentration up to $\sim 10^{19}\text{cm}^{-3}$ displayed in Ref. 44. The Mott criterion given by $n_c^{1/3} a_B \approx 0.25$ where a_B is the effective Bohr radius (given by $a_0 \frac{\varepsilon(0)}{m^*/m_0}$) and n_c the critical carrier density[52] gives n_c around $3 \times 10^{18}\text{cm}^{-3}$, meaning our absorption onset only minimally deviates from the fundamental band gap (from band filling effects). Indeed, our semiconductor statistics calculations, assuming a band edge effective mass of 0.28m_0 [Refs 53–55] and a nonparabolic conduction, band[56] indicate that for Ga_2O_3 with a carrier density of 6×10^{18} cm^{-3} the Fermi level is about 30 meV (0.03 eV) above the conduction band minimum (CBM). That is, the bulk CBM is essentially at the Fermi level. Therefore, given the measured band gap of about 4.68 eV, this indicates β-Ga_2O_3 ($\bar{2}01$) goes from downward to upward surface band bending as a function of in situ annealing. That is, the as received β-Ga_2O_3 ($\bar{2}01$) surface exhibits an electron accumulation layer which transforms into an electron depletion layer as the annealing treatment progresses. In order to illustrate the band bending and charge density as a function of depth quantitatively, the Poisson equation has been solved within the modified Thomas-Fermi approximation (MTFA),[57,58] with a nonparabolic conduction band, as described elsewhere.[56,59]

Fig. 3(a) and (b) shows the calculated band bending before and after annealing for the β-Ga_2O_3 ($\bar{2}01$) surface, and the associated electron density plots as a function of depth respectively. For the unannealed β-Ga_2O_3, the 0.24 eV downward band bending is associated with a corresponding accumulation of electrons in the near-surface region with a sheet electron density of 5×10^{12} cm^{-2}. For In_2O_3, weak conduction band emission was observed below the Fermi level in photoemission spectra.[6,60] However, in that case the surface sheet density was an order of magnitude higher than observed here for Ga_2O_3, explaining the absence of this feature in Fig. 1. The other charge profile shown in Fig. 3(a) is for the 0.26 eV upward band bending and surface electron depletion present after annealing at 800°C for 2 hours. The corresponding acceptor surface state density is 3.8×10^{12} cm^{-2}. The band bending as a function of annealing treatment is shown in Fig. 3(c) and is also correlated with the relative strength of the hydroxyl contribution to the O 1*s* spectrum, as discussed below. The uncertainty in the absolute band bending values is ± 0.22 eV due to the aforementioned uncertainties in the band gap and in determining the VBM position. However, the change in band bending is independent of the band gap and, between the as-received surface and after 800°C annealing, is 0.50 ± 0.14 eV using the VBM positions with their ± 0.10 eV uncertainty or 0.50 ± 0.07 eV using the core-level positions with their ± 0.05 eV uncertainty. The uncertainty in the band bending value would be much smaller than ± 0.22 eV with a less conservative estimate of the band gap than the ± 0.2 eV uncertainty stated here. Fig. 3(d) compares the natural band alignment and bulk interstitial H transition levels of Ga_2O_3 with other metal oxide semiconductors and will be discussed further below.

In order to confirm the changes in the surface electronic properties as a function of annealing and to investigate their origin, core level XPS spectra were also recorded. Fig. 4(a)-(d) shows XPS survey and core level spectra for β-Ga_2O_3 after successive in-situ thermal annealing steps were performed to remove surface contamination. Starting from an unannealed sample (black spectra), 200°C temperature steps were performed for 30 mins up to 800°C, which was also done for 2 hours (red spectra). All survey spectra possess only gallium, oxygen and carbon lines. No peaks related to Sn could be discerned due to the low concentration of Sn in the samples ($\sim 6 \times 10^{18}$ cm^{-3}), well below the detection limit. As successive annealing steps are completed, Ga and O related peaks are seen to increase in intensity, whilst C related peaks are greatly reduced, indicating the removal of contamination from the surface. This is more clearly seen in the core level spectra in Fig. 4(b) C 1*s*, (c) O 1*s* and (d) Ga 2*p*. The C 1*s* peak reduced in intensity after each annealing step up to 800°C where it could not be reduced further. Annealing at a higher temperature (1000°C) caused another carbon species to develop on the surface, possibly as a result of carbon reacting with Ga_2O_3. All core level peaks shifted to lower binding energy after each cleaning step, indicating changes in the surface electronic properties of the material occurring as a result of the surface cleaning.

This energy shift is investigated in more detail by peak fitting of the O 1*s* and Ga 2*p*

core levels as shown for the unannealed and maximally annealed crystal in Fig. 5. The O 1s spectra prior to cleaning (top) and after a 2 hour 800°C cleaning cycle (bottom) can be seen in Fig. 5(a). Both spectra were fitted using a Shirley background and Voigt line shapes. The spectrum possessed a strong component with a high binding energy shoulder. The main component is associated with O bonded to Ga at 532.2 eV, with a shoulder component 1.3 eV higher in binding energy, which is commonly associated with a hydroxyl (-OH) group.[61–65] In this case, this is likely due to H adatoms bonding to O atoms on the Ga_2O_3 surface. Subsequent annealing reduces and then removes the shoulder component completely and a binding energy shift of ∼0.7 eV to lower energy (531.6 eV) is observed. The FWHM of the O-Ga O 1s component remained the same (1.2 eV) before and after annealing, suggesting no new chemical species is formed. The binding energy shift of the O-Ga peak is associated with the change in the surface electronic properties resulting from the hydroxyl groups being removed from the surface. This correlation between the relative intensity of the hydroxyl component of the O 1s peak and the band bending is apparent in Fig. 3(c).

This suggests that the downward band bending and electron accumulation is due to the hydrogen on the surface. That is, the adsorbed hydrogen on the surface acts as an extrinsic source of positively charged donor surface states which provide the electrons in the accumulation layer. As the hydrogen is desorbed by annealing, the surface donor density decreases along with the downward band bending, and all the core levels shift accordingly. This effect has been seen previously in ZnO.[17,18] Indeed this is seen in Fig. 5(b) where the Ga $2p_{3/2}$ peak shifts after cleaning by the same amount also (from 1119.3 eV to 1118.6 eV with no change in the FWHM of 1.5 eV).

As the annealing steps progress, the initial decrease in the amount of downward band bending is followed by the development and then increase of upward band bending and surface electron depletion. The greatest upward band bending of 0.26 eV occurs when the hydroxyl component of the O 1s spectrum is absent after annealing at 800°C. This type of behavior has also been reported for polar ZnO surfaces.[16–18] These results suggest that electron depletion is the 'natural' surface space charge state of Ga_2O_3 surfaces. This corresponds to the presence of occupied negatively-charge acceptor-type intrinsic surface states.

Having electron depletion at the surface of moderately doped n-type Ga_2O_3 with roughly coincident bulk CBM and Fermi level, is consistent with the so-called charge neutrality level (CNL) lying below the CBM. The CNL, otherwise referred to as the Fermi level stabilization energy (of the amphoteric defect model[66,67]) or branch point energy,[68] is the energy at which the surface states change from being predominantly donor-like below the CNL, to being predominantly acceptor-like above the CNL.[10,13] Indeed, as shown in Fig. 3(d), the natural band alignments of the metal oxides indicate that CNL lies about 0.6 eV below the CBM for Ga_2O_3. Such a position high in the band gap and relatively close to the CBM for such a wide band gap material is consistent with other reported properties of Ga_2O_3. These include its n-type dopability,[69] the ability to form Schottky barriers at metal/Ga_2O_3 interfaces,[69] the sensitivity of surface conductivity to gas adsorption,[32] and the decrease in conductivity upon particle irradiation of already n-type material.[70]

However, a possible contradiction is presented by the bulk donor behaviour of interstitial hydrogen, H_i, in n-type Ga_2O_3. If the Fermi level is above the CNL, it would be expected that H_i would act as compensating acceptors. This is because for H_i configurations that involve disrupting the cation-anion bond, the H_i $\epsilon(+/-)$ transition level, corresponds to a transition between anion- and cation-derived dangling bond states and so is very close to the CNL.[10,71,72] But H_i have been shown to act exclusively as shallow donors in Ga_2O_3 from theory[73] and studies of the electronic analog muonium.[29] This apparent contradiction is resolved when the very different nature of the bonding of H_i in Ga_2O_3 compared to most other metal oxides is considered. The bonding environment of the O atoms in Ga_2O_3 results in O lone-pairs that may capture H_i and form favorable shallow donors without much influence on the lattice (bottom panels of Fig. 6). This is a phenomenon also exhibited by SnO_2. In the spirit of the usual relationship between the CNL and the behavior of H_i in

other materials, these lone-pair H_i^+ configurations for Ga_2O_3 and SnO_2 do not probe anion- and cation-derived dangling bond states and so their H_i transition level (denoted ϵ'(+/-) in Fig. 3(d)) does not correspond to the CNL for these materials. But, if we instead consider higher-formation energy H_i^+ configurations that disrupt the bonding and lead to cation dangling bonds (top panels of Fig. 6), we find the H_i ϵ(+/-) transition level[71] falls 0.51 eV below the CBM for Ga_2O_3, in good agreement with the experimental findings here and the CNL depicted 0.6 eV below the CBM in Fig. 3(d). (For SnO_2, we find that a bond-center H_i^+ configuration that probes Sn dangling bond energies yields a H_i ϵ(+/-) transition level 0.48 eV above the CBM, which is also qualitatively and quantitatively in good agreement with previous studies.[74])

In conclusion, the type and magnitude of band bending at the $(\bar{2}01)$ surface of β-Ga_2O_3 was determined for the as-entered and annealed crystal from valence band and core level XPS measurements combined with hybrid DFT valence band calculations. The surface of the as-entered Ga_2O_3 crystal is found to be terminated by O-H groups, resulting in downward band bending of 0.24 eV and electron accumulation with a sheet density of $\sim 5 \times 10^{12}$ cm^{-3}. Cleaning the surface by annealing and removing the adsorbed hydrogen results in a transition from electron accumulation to depletion with upward band bending of 0.26 eV. The observation of electron accumulation at uncleaned and even moderately annealed Ga_2O_3 surfaces has been previously overlooked and the extent of depletion overestimated. This is due in different cases either to use of the wrong band gap energy and/or to an over-reliance upon linear extrapolation of the valence band leading edge for the determination of the VBM position with respect to the Fermi level. These findings are consistent with the charge neutrality level lying $\sim$0.6 eV below the CBM, which is in line with other reported properties of Ga_2O_3 and also our calculated ϵ(+/-) transition level for bond disrupting H_i configurations.

JENS acknowledges funding through the Engineering and Physical Sciences Research Council (EPSRC) Centre for Doctoral Training in New and Sustainable Photovoltaics (EP/L01551X/1). TDV and VRD acknowledge funding from EPSRC grant no. EP/N015800/1. This work was partially performed under the auspices of the U.S. DOE by Lawrence Livermore National Laboratory under contract DE-AC52-07NA27344, and supported by the Critical Materials Institute, an Energy Innovation Hub funded by the U.S. DOE, Office of Energy Efficiency and Renewable Energy, Advanced Manufacturing Office. This work was also supported by the Air Force Office of Scientific Research under award number FA9550-18-1-0024. TDV acknowledges discussions with Novel Crystal Technology, Inc., Tamura Corporation.

[1]N. Ueda, H. Hosono, R. Waseda, and H. Kawazoe, Appl. Phys. Lett. **71**, 933 (1997).
[2]M. Rebien, W. Henrion, M. Hong, J. P. Mannaerts, and M. Fleischer, Appl. Phys. Lett. **81**, 250 (2002).
[3]Y. Kokubun, K. Miura, F. Endo, and S. Nakagomi, Appl. Phys. Lett. **90**, 031912 (2007).
[4]M. Ogita, N. Saika, Y. Nakanishi, and Y. Hatanaka, Appl. Surf. Sci. **142**, 188 (1999).
[5]M. Higashiwaki, K. Sasaki, H. Murakami, Y. Kumagai, A. Koukitu, A. Kuramata, T. Masui, and S. Yamakoshi, Semicond. Sci. Technol. **31**, 034001 (2016).
[6]P. D. C. King, T. D. Veal, F. Fuchs, C. Y. Wang, D. J. Payne, A. Bourlange, H. Zhang, G. R. Bell, V. Cimalla, O. Ambacher, R. G. Egdell, F. Bechstedt, and C. F. McConville, Phys. Rev. B **79**, 205211 (2009).
[7]S. K. Vasheghani Farahani, T. D. Veal, J. J. Mudd, D. O. Scanlon, G. W. Watson, O. Bierwagen, M. E. White, J. S. Speck, and C. F. McConville, Phys. Rev. B **90**, 155413 (2014).
[8]L. F. J. Piper, L. Colakerol, P. D. C. King, A. Schleife, J. Zúñiga-Pérez, P.-A. Glans, T. Learmonth, A. Federov, T. D. Veal, F. Fuchs, V. Muñoz-Sanjosé, F. Bechstedt, C. F. McConville, , and K. E. Smith, Phys. Rev. B **78**, 165127 (2008).
[9]M. W. Allen, C. H. Swartz, T. H. Myers, T. D. Veal, C. F. McConville, and S. M. Durbin, Phys. Rev. B **81**, 075211 (2010).
[10]P. D. C. King, T. D. Veal, P. H. Jefferson, J. Zúñiga-Pérez, V. Muñoz-Sanjosé, and C. F. McConville, Phys. Rev. B **79**, 035203 (2009).
[11]P. D. C. King, T. D. Veal, D. J. Payne, A. Bourlange, R. G. Egdell, and C. F. McConville, Phys. Rev. Lett. **101**, 116808 (2008).
[12]I. Mahboob, T. D. Veal, C. F. McConville, H. Lu, and W. J. Schaff, Phys. Rev. Lett. **92**, 036804 (2004).
[13]P. D. C. King, T. D. Veal, P. H. Jefferson, S. A. Hatfield, L. F. J. Piper, C. F. McConville, F. Fuchs, J. Furthmller, F. Bechstedt, H. Lu, and W. J. Schaff, Phys. Rev. B **77**, 045316 (2008).
[14]P. D. C. King and T. D. Veal, J. Phys. Condens. Matter. **23**, 334214 (2011).

[15] G. Heiland and P. Kunstmann, Surf. Sci. **13**, 72 (1969).
[16] R. Heinhold and M. W. Allen, J. Mater. Res. **27**, 2214 (2012).
[17] R. Heinhold, G. T. Williams, S. P. Cooil, D. A. Evans, and M. W. Allen, Phys. Rev. B **88**, 235315 (2013).
[18] R. Heinhold, S. P. Cooil, D. A. Evans, and M. W. Allen, J. Phys. Chem. C **118**, 24575 (2014).
[19] M. Batzill and U. Diebold, Prog. Surf. Sci. **79**, 47 (2005).
[20] T. Nagata, O. Bierwagen, M. E. White, M.-Y. Tsai, and J. S. Speck, J. Appl. Phys. **107**, 033707 (2010).
[21] S. J. Pearton, J. Yang, P. H. Cary, J. K. F. Ren, M. J. Tadjer, and M. A. Mastro, Appl. Phys. rev. **5**, 011301 (2018).
[22] A. Navarro-Quezada, S. Alamé, N. Esser, J. Furthmüller, F. Bechstedt, Z. Galazka, D. Skuridina, and P. Vogt, Phys. Rev. B **92**, 195306 (2015).
[23] A. Navarro-Quezada, Z. Galazka, S. Alamé, D. Skuridina, P. Vogt, and N. Esser, Appl. Surf. Sci. **349**, 368 (2015).
[24] T. C. Lovejoy, R. Chen, C. Zheng, E. G. Villora, K. Shimamura, H. Yoshikawa, Y. Tamashita, S. Ueda, K. Kobayashi, S. T. Dunham, F. S. Ohuchi, and M. A. Olmstead, Appl. Phys. Lett. **100**, 181602 (2012).
[25] M. Mohamed, I. Unger, C. Janowitz, R. Manzke, Z. Galazka, R. Uecker, and R. Fornari, J. Phys. Conf. Ser. **286**, 012027 (2011).
[26] T. C. Lovejoy, E. N. Yitamben, N. Shamir, J. Morales, E. G. Villora, K. Shimamura, S. Zheng, F. S. Ohuchi, and M. A. Olmstead, Appl. Phys. Lett. **94**, 081906 (2009).
[27] M. Mohamed, C. Janowitz, I. Unger, R. Manzke, Z. Galazka, R. Uecker, R. Fornari, J. R. Weber, J. B. Varley, and C. G. Van de Walle, Appl. Phys. Let. **97**, 211903 (2010).
[28] L. F. J. Piper, A. R. H. Preston, A. Fedorov, S. W. Cho, A. DeMasi, and K. E. Smith, Phys. Rev. B **81**, 233305 (2010).
[29] P. D. C. King, I. McKenzie, and T. D. Veal, Appl. Phys. Lett. **96**, 062110 (2010).
[30] J. B. Varley, H. Peelaers, A. Janotti, and C. G. Van de Walle, J. Phys.: Condens. Matter **23**, 334212 (2011).
[31] H. Li and J. Robertson, J. Appl. Phys. **115**, 203708 (2014).
[32] M. Fleischer, J. Giber, and H. Meixner, Appl. Phys. A **54**, 560 (1992).
[33] H. Geistlinger, Sensors and Actuators B **18-19**, 125 (1994).
[34] H. Aida, K. Nishiguchi, H. Takeda, N. Aota, K. Sunakawa, and Y. Yaguchi, Jpn. J. Appl. Phys. **47**, 8506 (2008).
[35] T. J. Whittles, L. A. Burton, J. M. Skelton, A. Walsh, T. D. Veal, and V. R. Dhanak, Chem. Mater. **28**, 3718 (2016).
[36] S. Ahn, F. Ren, E. Patrick, M. E. Law, and S. J. Pearton, ECS J. Solid state Sci. Technol. **6**, Q3026 (2017).
[37] S. Ahn, F. Ren, E. Patrick, M. E. Law, S. J. Pearton, and A. Kuramata, Appl. Phys. Lett. **109**, 242108 (2016).
[38] J. Heyd, G. E. Scuseria, and M. Ernzerhof, J. Chem. Phys **118**, 8207 (2003).
[39] J. Heyd, G. E. Scuseria, and M. Ernzerhof, J. Chem. Phys. **124**, 219906 (2006).
[40] P. E. Blöchl, Phys. Rev. B **50**, 17953 (1994).
[41] G. Kresse and J. Furthmüller, Phys. Rev. B **54**, 11169 (1996).
[42] G. Kresse and J. Furthmüller, Comput. Mater. Sci. **6**, 15 (1996).
[43] H. Peelaers, J. B. Varley, J. S. Speck, and C. G. Van de Walle, Appl. Phys. Lett. **112**, 242101 (2018).
[44] S. Rafique, L. Han, S. Mou, and H. Zhao, Opt. Mater. Express **7**, 3561 (2017).
[45] C. Freysoldt, J. Neugebauer, and C. G. Van de Walle, Phys. Rev. Lett. **102**, 016402 (2009).
[46] M. E. Ingebrigtsen, J. B. Varley, A. Y. Kuznetsov, B. G. Svensson, G. Alfieri, A. Mihaila, U. Badstübner, and L. Vines, Appl. Phys. Lett. **112**, 042104 (2018).
[47] J. Scofield, "Theoretical photoionization cross sections from 1 to 1500 keV." Tech. Rep. (Divison of Technical Information Extension, U.S. Atomic Energy Commission, 1973).
[48] E. A. Kraut, R. W. Grant, J. R. Waldrop, and S. P. Kowalczyk, Phys. Rev. Lett. **44**, 1620 (1980).
[49] H. Fu, H. Chen, X. Huang, I. Baranowski, J. Montes, T.-H. Yang, and Y. Zhao, IEEE Trans. Electron Devices **65**, 3507 (2018).
[50] S.-M. Sun, W.-J. Liu, Y.-P. Wang, Y.-W. Huan, Q. Ma, B. Zhu, S.-D. Wu, W.-J. Yu, R.-H. Horng, C.-T. Xia, Q.-Q. Sun, S.-J. Ding, and D. W. Zhang, Appl. Phys. Lett. **113**, 2018 (2018).
[51] C. Sturm, R. Schmidt-Grund, C. Kranert, J. Furthmuller, F. Bechstedt, and M. Grundmann, Phys. Rev. B **94**, 035148 (2016).
[52] P. P. Edwards and M. J. Sienko, J. Am. Chem. Soc **103**, 2967 (1981).
[53] H. Peelaers and C. G. Van de Walle, Appl. Phys. Lett. **111**, 182104 (2017).
[54] A. Mock, R. Korlacki, C. Briley, V. Darakchieva, B. Monemar, Y. Kumagai, K. Goto, M. Higashiwaki, and M. Schubert, Phys. Rev. B **96**, 245205 (2017).
[55] S. Knight, A. Mock, R. Korlacki, V. Darakchieva, B. Monemar, Y. Kumagai, K. Goto, M. Higashiwaki, and M. Schubert, Appl. Phys. Lett. **112**, 012103 (2018).
[56] T. D. Veal, L. F. J. Piper, W. J. Schaff, and C. F. McConville, J. Cryst. Growth **288**, 268 (2006).
[57] G. Paasch and H. Übensee, Phys. Status Solidi B **113**, 165 (1982).
[58] J.-P. Zöllner, H. Übensee, G. Paasch, T. Fiedler, and G. Gobsch, Phys. Status Solidi B **134**, 837 (1986).
[59] P. D. C. King, T. D. Veal, and C. F. McConville, Phys. Rev. B **77**, 125305 (2008).
[60] K. H. L. Zhang, R. G. Egdell, F. Offi, S. Iacobucci, L. Petaccia, S. Gorovikov, and P. D. C. King, Phys. Rev. Lett. **110**, 056803 (2013).

[61]M. F. Al-Kuhaili, S. M. A. Durrani, and E. E. Khawaja, Appl. Phys. Lett. **83**, 4533 (2003).
[62]T. Lay, Y. Liaoa, W. Hung, M. Hong, J. Kwo, and J. Mannaerts, J. Cryst. Growth **278**, 624 (2005).
[63]C. V. Ramana, E. J. Rubio, C. D. Barraza, A. M. Gallardo, S. McPeak, S. Kotru, and J. T. Grant, J. Appl. Phys. **115**, 043508 (2014).
[64]E. J. Rubio, T. E. Mates, S. Manandhar, M. Nandasiri, V. Shutthanandan, and C. V. Ramana, J. Phys. Chem. C **120**, 26720 (2016).
[65]J. Sheng, E. J. Park, B. Shong, and J.-S. Park, ACS Appl. Mater. Interfaces **9**, 23934 (2017).
[66]W. Walukiewicz, Phys. Rev. B **37**, 4760 (1988).
[67]W. Walukiewicz, Appl. Phys. Lett. **54**, 2094 (1989).
[68]J. Tersoff, Phys. Rev. Lett. **52**, 465 (1984).
[69]H. von Wenckstern, Adv. Electron. Mater. **3**, 1600350 (2017).
[70]L. Vines, C. Bhoodoo, H. von Wenckstern, and M. Grundmann, J. Phys.: Condens. Matter **30**, 025502 (2018).
[71]C. G. Van de Walle and J. Neugebauer, Nature **423**, 626 (2003).
[72]P. D. C. King, R. L. Lichti, Y. G. Celebi, J. M. Gil, R. C. Vilão, H. V. Alberto, J. Piroto Duarte, D. J. Payne, R. G. Egdell, I. McKenzie, C. F. McConville, S. F. J. Cox, and T. D. Veal, Phys. Rev. B **80**, 081201(R) (2009).
[73]J. B. Varley, J. R. Weber, A. Janotti, and C. G. Van de Walle, Appl. Phys. Lett. **97**, 142106 (2010).
[74]B. Falabretti and J. Robertson, J. Appl. Phys. **102**, 123703 (2007).
[75]M. N. Amini, R. Saniz, D. Lamoen, and B. Partoens, J. Appl. Phys. **110**, 063521 (2011).
[76]S. Limpijumnong, P. Reunchan, A. Janotti, and C. G. Van de Walle, Phys. Rev. B **80**, 193202 (2009).
[77]T. D. Veal, P. D. C. King, S. A. Hatfield, L. R. Bailey, C. F. McConville, B. Martel, J. C. Moreno, E. Frayssinet, F. Semond, and J. Zúñiga-Pérez, Appl. Phys. Lett. **93**, 202108 (2008).
[78]V. N. Brudnyi, S. N. Grinyaev, and N. G. Kolin, Semiconductors **37**, 537 (2003).
[79]C. Janowitz, V. Scherer, M. Mohamed, A. Krapf, H. Dwelk, R. Manzke, Z. Galazka, R. Uecker, K. Irmscher, R. Fornari, M. Michling, D. Schmeisser, J. R. Weber, J. B. Varley, and C. G. Van de Walle, New J. Phys **13**, 085014 (2011).

Figure captions

Figure 1: Valence band photoemission spectra and DFT valence band total DOS with and without instrumental and lifetime broadening applied for β-Ga_2O_3 (a) as entered, and (b) after annealing at 800°C for 2 hours. (c) the evolution of valence band spectra under subsequent annealing cycles at increasing temperatures.

Figure 2: Optical absorption as a function of photon energy for β-Ga_2O_3 with the [010] plane upward (red) and alternately the [102] plane facing the incoming light (black).

Figure 3: Poisson-MTFA calculations of (a) the band bending and (b) carrier density profiles in the electron accumulation (blue) and depletion (red) surface layers for β-Ga_2O_3 before and after cleaning. (c) The β-Ga_2O_3 surface band bending and the relative contribution of the hydroxyl component of the O 1s spectrum as a function of annealing temperature. The annealing temperature of 20°C on the upper x-axis represents the unannealed sample. The lines between points are a guide to the eye. (d) Band line-up with respect to the charge neutrality level for β-Ga_2O_3 compared to that of other metal oxide semiconductors. The CNL for β-Ga_2O_3, In_2O_3,[6] ZnO[77] and CdO[10] are determined from valence band offsets from particle irradiation studies of other materials[78] and from calculations for SnO_2.[74] The CBM shown for CdO is for the Γ point rather than the indirect CBM at the the L point. The ϵ(+/-) transition levels for H_i configurations which involve disrupting the cation-anion bond are shown as dotted orange lines for β-Ga_2O_3 (0.51 eV below the CBM - this work), In_2O_3 (0.53 eV above the CBM),[76] ZnO (0.40 eV above the CBM),[71] SnO_2 (0.48 eV above the CBM for the bond disrupting H_i^+ configuration - this work), and CdO (0.43 eV above the CBM).[75] Also shown, as purple dotted lines, are the ϵ'(+/-) transition levels for H_i configurations that involve O lone-pairs capturing H_i which are the lowest formation energy for β-Ga_2O_3 (ϵ'(+/-) at 4.90 eV above the VBM,[73] corresponding to 0.22 eV above the CBM for our room temperature band gap of 4.68 eV) and SnO_2 (ϵ'(+/-) at 1.53 eV above the CBM).[30]

Figure 4: β-Ga_2O_3 XPS spectra following thermal annealing steps at 200, 400, 600 and 800°C for 30 minutes and finally for 2 hrs at 800 °C showing (a) wide survey scan with visible peaks labeled. (b) C 1s core-level, (c) O 1s core-level and (d) Ga 2p core level doublets, all demonstrating a binding energy shift to lower energy upon surface cleaning up to 800°C. The binding energy scale is referenced to the Fermi level.

Figure 5: (a) O 1s and (b) Ga 2$p_{3/2}$ XPS core level peaks and curve fitting for both unannealed (as entered) samples and following a 2 hour 800°C annealing cycle.

Figure 6: Comparison of H_i^+ configurations used in the alignment for (a) rutile SnO_2 and (b) monoclinic β-Ga_2O_3. The top panels represents the bond-center (a) or anti-bonding (b) configurations that disrupt the host bonding. The broken Ga-O bond in (b) is represented by a dashed line. The bottom panels represent the lowest energy configurations for H_i^+ in these structures, but they do not probe the cation-anion bonds and instead occupy anion-derived lone-pairs.

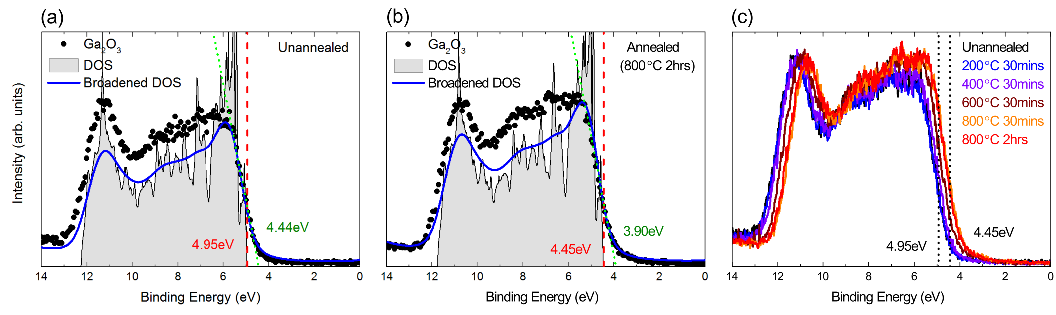

FIG. 1.

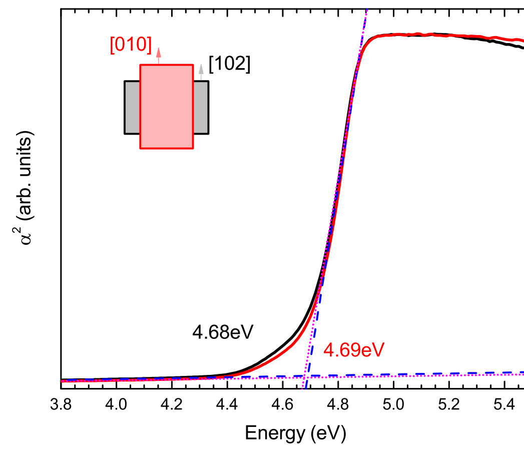

FIG. 2.

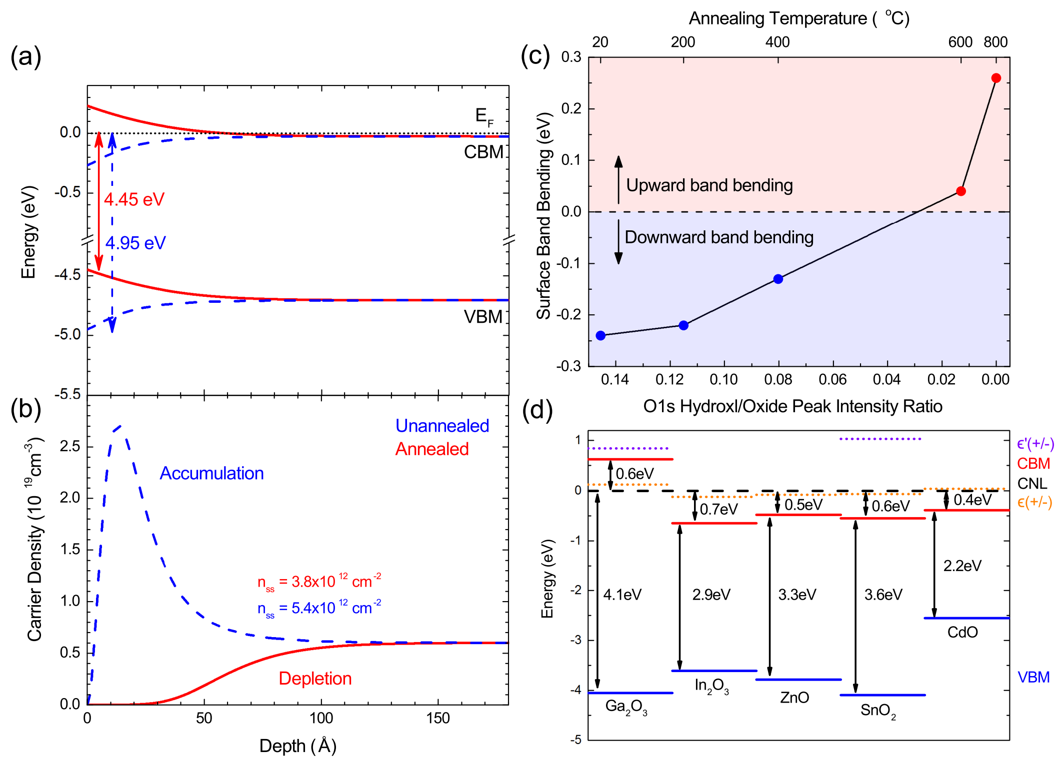

FIG. 3.

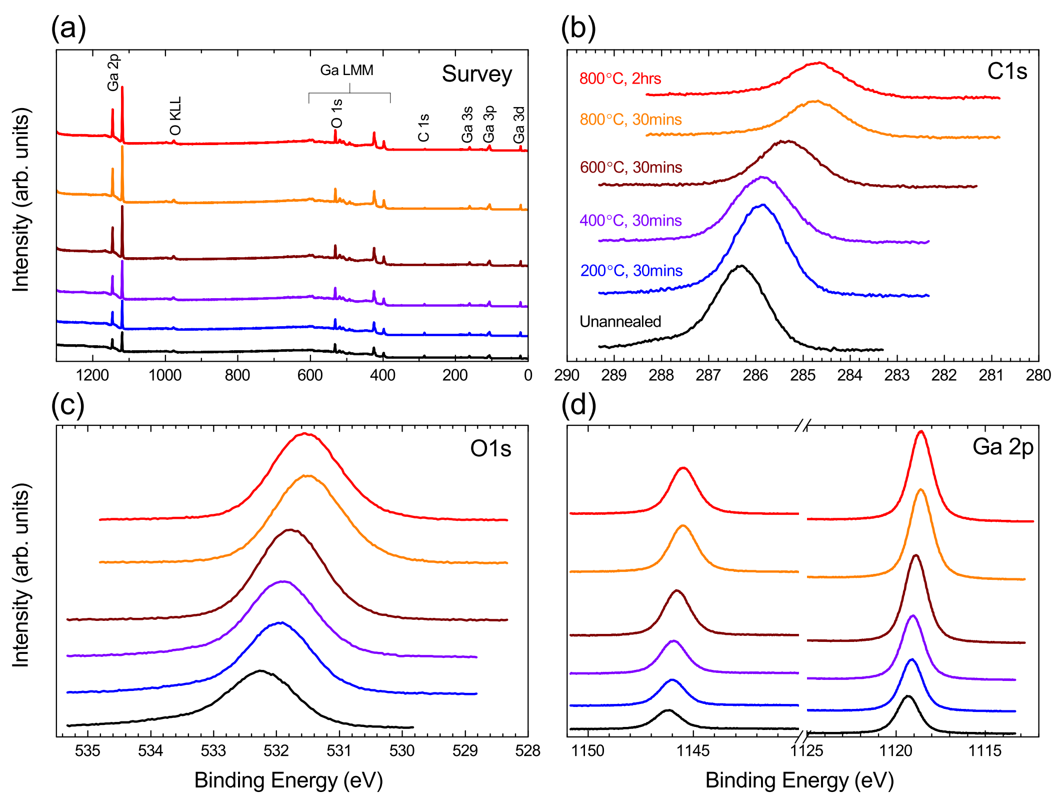

FIG. 4.

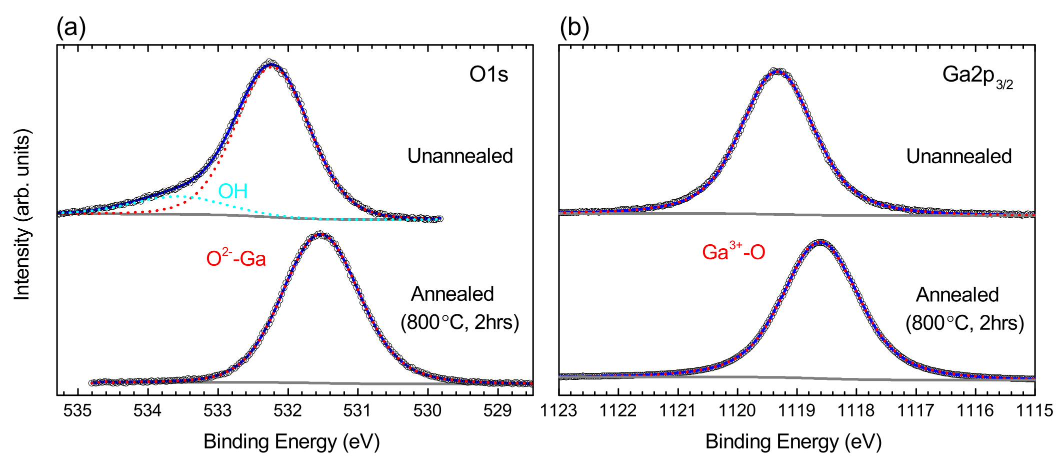

FIG. 5.

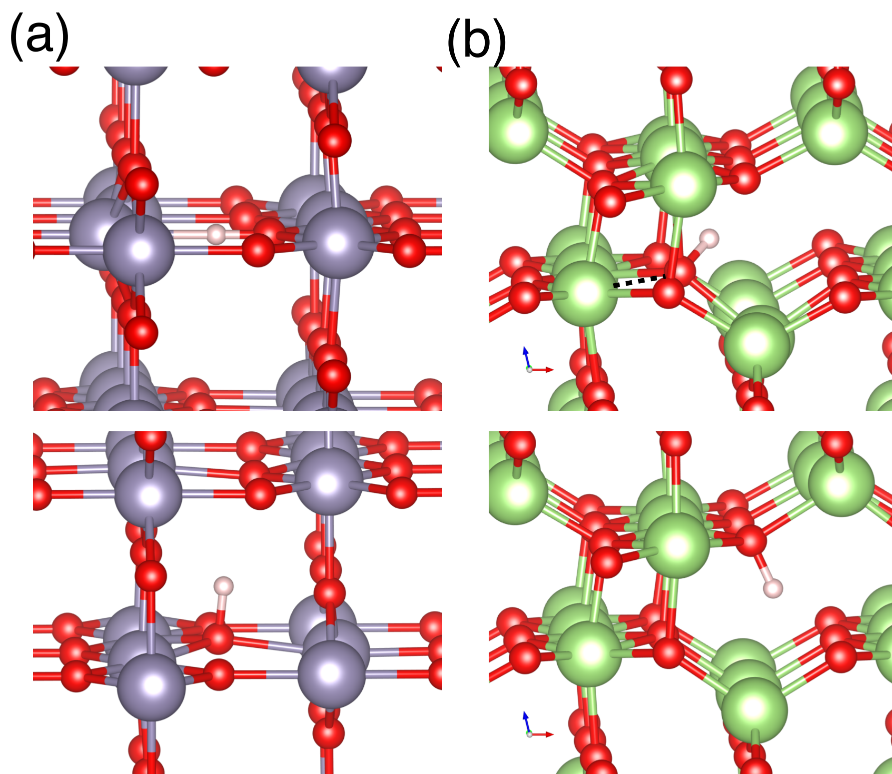

FIG. 6.